CRYSTAL GROWTH & DESIGN

pubs.acs.org/crystal

Article

The Ag_{10} Cluster-Based One-Dimensional Silver-Thiolate Assembly: Structural Architecture and Photophysical Properties

Published as part of Crystal Growth & Design virtual special issue "Honoring Professor Jagadese J. Vittal and his Contributions to Functional Molecular Crystals".

Rahul Ramachandran Manikkoth, Priyadarshini Baidya,[§] Sreehari Surendran Rajasree,[§] Priyanka Chandrashekar,[§] Manju P. Maman, Pravas Deria,* and Sukhendu Mandal*

Cite This: *Cryst. Growth Des.* 2024, 24, 4213−4219

Read Online

ACCESS | Metrics & More | Article Recommendations | Supporting Information

ABSTRACT: Silver clusters create the most aesthetic structures compared with other group-11 metal systems, but structural instability often hinders probing their in-depth optoelectronic properties. Assembling these clusters to higher dimensions provides the needed stability and creates a platform to underscore the dimensionality-dependent photophysical properties. Here, we synthesized a one-dimensional ladder-like architecture by interconnecting $[Ag_{10}(^tBuS)_6(CF_3COO)_6]^{2-}$ cluster through a 4,4′-trimethylene dipyridine linker. The 1D chains are stacked in an *AAAA* fashion in the *c* direction and an *ABAB* fashion in the *a* direction to form a three-dimensionally supramolecular extended solid. Steady-state and transient emission experiments probed at room temperature and 77 K showed the presence of triplets with lifetime >50 μs at 77 K and room temperature reverse intersystem crossing. The detailed photophysical study proposed that this one-dimensional assembly acquires a large window of radiative recombination and its dynamics as a function of external stimuli.

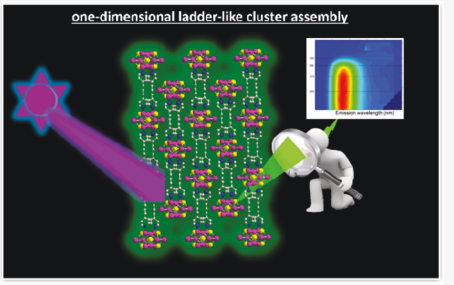

1. INTRODUCTION

Metal nanoclusters (NCs), consisting of a few to several hundred atoms, have garnered significant interest as a captivating class of materials due to their precise atomic arrangement and size-dependent properties. These subnanometer-sized clusters exhibit distinctive electronic, optical, and catalytic properties with respect to their bulk counterparts.[1,2] Photoluminescence (PL), one of their intriguing properties, holds great promise for various applications such as chemical sensing, bioimaging, cell labeling, phototherapy, and drug delivery. The contemporary surge in ligand-protected atom-precise metal clusters to exploit their unique photophysical features critically requires implementation strategies to improve their stability and tune their photonic properties through electronic modulation.[3−6] Among these, silver chalcogenolate clusters entice interest due to their elegant structures and intriguing optoelectronic properties.[7−9] However, in-depth study of silver clusters is often hindered due to their instability towards oxidation. Moreover, the small size of the metal NCs makes these difficult to handle for application purposes.[10] Assembling these molecular clusters into higher dimensions is expected to be beneficial through structural hierarchy suppressing the dynamics of labile bonds.[10,11] Based on analogous metal−organic frameworks,[12,13] we envision that the assembly of these molecular clusters into solid frameworks will provide a viable route to tune their optoelectronic properties to meet specific applications.[14−16] Cluster-assembled materials (CAM) are constructed by interconnecting the clusters as nodes through multitopic linkers.[10,17−20] This is aided by the unique geometrical architecture that can lead to frameworks known as CAM with unique architecture and electronic structures.[10,11,21−24] Supramolecular structures arising from noncovalent interactions of the ligands, such as C−H···π, π−π, H-bonding, van der Waals, etc., can cause these frameworks to assemble in different dimensionality.[22] Linkers of different structures and symmetry connect silver clusters into one-, two-, and three-dimensional patterns by the coordination assembly.[10] While most of the assemblies studied are either 3D or 2D, it is necessary to explore the intercluster interaction in less complicated 1D structures that are currently limited.[11] Photophysical developments with CAMs require an enriched synthetic toolkit for specific structures with desired dimensionality that can tackle interfering parameters like the size of the linker, geometry, cluster symmetry and directionality, and tolerance of synthetic conditions.[11,23−25]

Received: March 2, 2024
Revised: April 18, 2024
Accepted: April 19, 2024
Published: April 30, 2024

Atom-precise silver clusters have been established to possess unique photophysical behaviors and if the emission at longer wavelengths is cluster-centered, it is predominantly attributed to the triplet emitting state.[25−29] Their optoelectronic properties are defined by their ligand-to-metal charge transfer (LMCT) mixed with metal-centered-based transitions and can be modulated by the compositional variation of the cluster itself. Previously, we have shown an Ag_{12} NC using monotopic pyridine and its corresponding 2D framework linked by the tritopic TmPyPB (1,3,5-tris(3-pyridyl-3-phenyl)benzene) linker; the change in their energy gap was found to be dictated by their assemblies or added dimensionality and thus creating a significant temperature-dependent emission behavior.[30] It is, therefore, intriguing to develop a systematic understanding of how added dimensionality exquisitely defines new materials that will enable light harvesting to generate usable long-lived excitons. Here, we have synthesized an assembly, Ag_{10}-cluster based one-dimensional structure constructed by interconnecting $[Ag_{10}(^tBuS)_6(CF_3COO)_6]^{2-}$ cluster units by the 4,4′-trimethylene dipyridine (TMD) linker designated as Ag_{10} CAM. Photophysical studies and transient emission profiles suggest that the material possesses a large tunable window of radiative recombination, and their dynamics are defined by external stimuli like temperature.

2. EXPERIMENTAL SECTION

2.1. Chemicals. Silver nitrate ($AgNO_3$), tertiary butyl thiol (^tBuSH), silver trifluoroacetate (CF_3COOAg), and 4,4′-trimethylene dipyridine (TMD) were procured from Sigma-Aldrich. HPLC grade solvents: methanol (MeOH), *N*,*N*-dimethylacetamide (DMAc), and triethylamine (Et_3N) were purchased from Spectrochem.

2.2. Synthesis of Silver *tert*-Butyl Thiol complex $[Ag^tBuS]_n$. To a solution of 3 mmol (510 mg) of $AgNO_3$ in 20 mL of MeOH, 3 mmol (338 μL) of tertiary butyl thiol was added while stirring. After 5 min of stirring, 1 mmol (139 μL) of Et_3N was added. The resultant white dispersion was stirred overnight (∼12 h) in a dark environment, and the white precipitate was isolated and washed with MeOH at least three times.

2.3. Synthesis of Ag_{10} CAM. A total of 0.125 mmol (24.7 mg) portion of the $[Ag^tBuS]_n$ complex and 0.1 mmol (22 mg) of CF_3COOAg were sequentially added to 3 mL of DMAc solvent in a glass vial and sonicated until soluble. Subsequently, 0.05 mmol (10 mg) of the 4,4′-trimethylene dipyridine (TMD) linker was dissolved separately in 1 mL of DMAc, which was then added dropwise through the sides of the vial to the previously prepared solution, and the whole mixture was allowed to crystallize in a dark environment for 3 days at room temperature to obtain colorless plate-like crystals (yield = 57.4% with respect to CF_3COOAg).

2.4. X-ray Crystallography. The single-crystal X-ray diffraction (SC-XRD) data for Ag_{10} CAM was collected on the Bruker Axs Kappa Apex II SC-XRD diffractometer with CCD detector using monochromated Mo Kα radiation (λ = 0.71073 Å). The crystal structure was solved by SHELXT 2014 and refined by the full matrix least-squares method using SHELXL 2018 present in the program suite WinGX (version 2014.1).[31−33] All non-hydrogen atoms were refined anisotropically, and hydrogen atoms were (positioned geometrically) refined isotropically using an olex2.[34]

2.5. Instrumentation. UV−vis spectroscopy was carried out on a UV-3800 SHIMADZU UV−vis/NIR spectrometer using a 3.5 mL cuvette. X-ray photoelectron spectroscopy (XPS) measurements were done using the Omicron nanotech instrument (Mg Kα radiation at 1253.6 eV). All binding energies were referenced to the neutral C 1s peak at 284.8 eV. Infrared (IR) spectra (with a spectral resolution of 4 cm^{-1}) were collected on a Shimadzu IR Prestige−21 FTIR spectrometer by using the KBr pellet method. Powder X-ray diffraction (PXRD) data were collected employing an X'pert PRO (PANalytics) powder diffractometer equipped with a Cu Kα (λ = 1.5405 Å) radiation source. Scanning electron microscopy (SEM) was carried out for morphological analysis using an FEI Nova NANOSEM 450. Steady-state photoluminescent spectra were collected with an Edinburg FS5 spectrofluorometer. Emission spectra and excitation−emission mapping were carried out in front face configuration, whereas absolute quantum yield (QY) was determined using a 150 mm $BaSO_4$ coated integrating sphere. Transient emission decay profiles were collected using an Edinburgh Lifespec II picosecond time-correlated single-photon counting (TCSPC) spectrophotometer equipped with a 403 nm pulsed diode laser (pulse width: 60 ps; IRF: 160 ps). Kinetic data were fitted with the F980 software. For steady-state measurements, the sample was loaded in a quartz capillary tube with the desired solvent (3× freeze−pump−thawed) inside the glovebox and sealed with Teflon tape. The singlet oxygen experiment on the powder sample was measured using a Horiba Jobin Yvon spectrofluorometer, and cryogenic equipment by a Janis VNF-100 cryostat with a temperature controller was used for the low-temperature measurements.

3. RESULTS AND DISCUSSION

The Ag_{10} CAM crystallized in monoclinic space group *C*2/*m* (no. 12) (Table S1 for crystallographic details). The

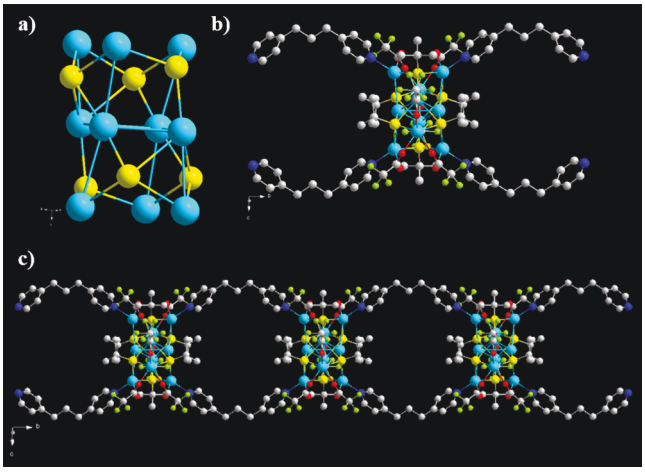

Figure 1. Structure of Ag_{10} CAM (a) $Ag_{10}S_6$ cluster core, (b) connectivity of the cluster with TMD linker, and (c) TMD linker with cluster producing one-dimensional ladder-type structure. Color code: Ag, sky blue; S, yello; O, red; F, light green; N, blue; C, gray. All H atoms are omitted for clarity.

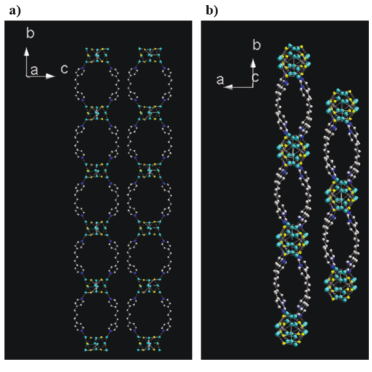

Figure 2. Crystal packing of Ag_{10} CAM, (a) one-dimensional structure stacked along *c* axis shows *AA* kind of stacking pattern, (b) one-dimensional structure along *a* axis shows *AB* stacking. Color code: Ag, sky blue; S, yellow; N, blue; C, gray.

https://doi.org/10.1021/acs.cgd.4c00322
Cryst. Growth Des. 2024, 24, 4213−4219

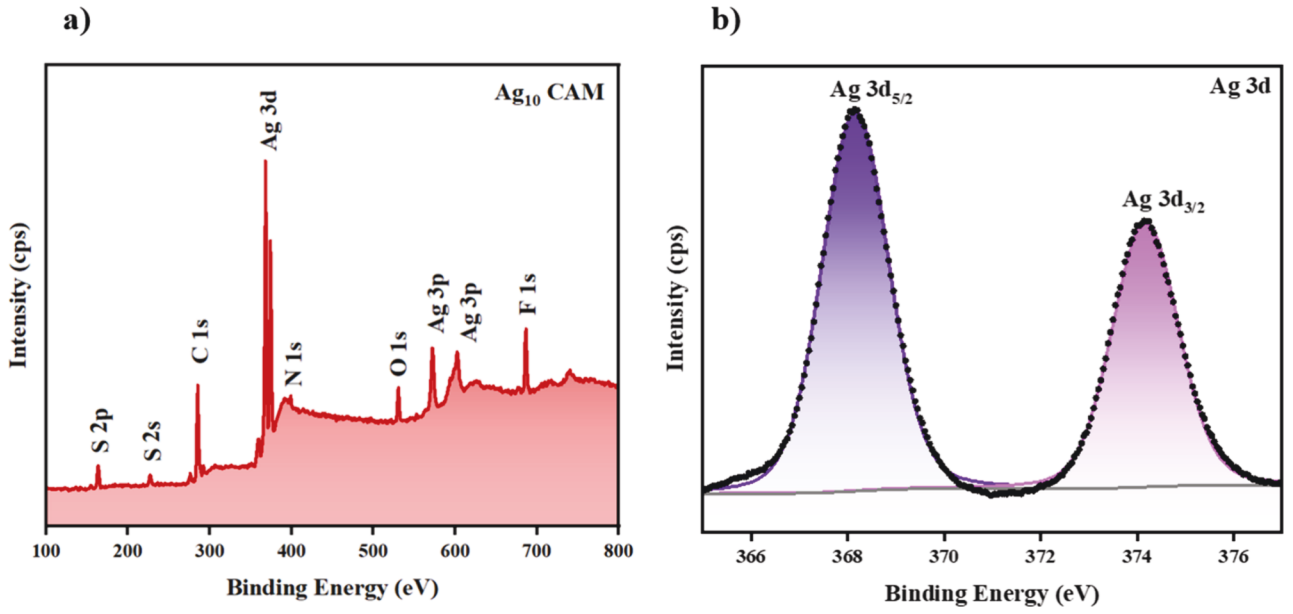

Figure 3. (a) XPS survey spectra and (b) deconvoluted XPS data of the silver.

compound has the formula $[Ag_{10}(^tBuS)_6(CF_3COO)_6(TMD)_2]^{2-}$, and the negative charge is balanced by extra-framework cation $[HNEt_3]^+$. The location of this cation was difficult to probe from the single crystal data due to the absorption of a myriad of heavy silver atoms. Characteristic features of N−H bands in infrared spectroscopic data supported the presence of protonated amine cation.

The Ag_{10} cluster/node is protected by tertiary butyl thiolate ($^tBuS^-$) and silver trifluoroacetate (CF_3COO^-) ligands, and each cluster node is linked to one another by two TMD linker forming a one-dimensional structure with ladder-type architecture (Figure 1). The distances between adjacent silver atoms fall in the range of 2.98−3.25 Å, which is smaller than the sum of the van der Waals radius of silver (3.44 Å), suggesting the presence of argentophilic interactions.[35,36] Structural details suggest that the $Ag_{10}S_6$ cluster contains a rhombic Ag_4 subunit sandwiched between two chair-shaped Ag_3S_3 subunits, linked to each other through argentophilic interaction and silver-thiolate bonds (Figure S1). Out of six S atoms, four of these bind to silver through the μ_4-η^1:η^1:η^1:η^1 coordination mode, with Ag−S bond distances of ∼2.36−2.74 Å, and the remaining two S atoms bind to silver through the μ_3-η^1:η^1:η^1 coordination mode, with Ag−S bond distances of ∼2.47 Å (Figure S2). The CF_3COO^- acts as a bidentate auxiliary ligand (Figure S3) with Ag−O bond distances ranging from 2.31 to 2.62 Å. Based on their coordination environment, the cluster unit consists of four different types of silver atoms. Ag (1) is five-coordinated, adopting a distorted capped tetrahedron geometry. Ag (2) and Ag (3) are six-coordinated with a distorted trigonal antiprism geometry. The Ag (4) is seven-coordinated and adopts a distorted bicapped pentagonal pyramidal geometry (Figure S4). The cluster node of Ag_{10} CAM structurally resembled the one previously reported pyridine protected $[Ag_{10}(^tBuS)_6(Py)_6(CF_3CO_2)_4]\cdot 3Py$, molecular cluster (Table S2 and Figures S5).[37] The change of N-based linker from pyridine to TMD is reflected in the structural dimensionality and respective bonding connectivity (see the SI).

Each Ag_{10} cluster unit is coordinated to four TMD linkers with Ag−N bond distances of ∼2.24 Å, with two TMD linkers connected via the Ag−N bond to each of the Ag_3S_3 chair-shaped subunits (Figure 1b). The two N atoms in the TMD connect adjacent Ag_{10} clusters, separated by 17.07 Å (Figure S6). This arrangement entails a 1D structure with a ladder-type architecture (Figure 1c and Figure S6). The 1D structures stack on top of each other in an *AAAA* fashion along the *c*-axis, each separated by 9.3 Å (Figure 2a). Whereas in the *a* direction, it shows *ABAB* stacking fashion, where the Ag_{10} cluster unit of the adjacent ladder-type architecture is found directly above the void formed by the three methylene groups of TMD to form a three-dimensionally supramolecular solid (Figure 2b, Figures S6 and S7). These *AB* stacks are separated by 15.7 Å (Figure S6).

The phase purity of the bulk crystalline material was verified by matching the experimental PXRD pattern of the powdered crystal with the simulated PXRD obtained from the crystal data (Figure S8). The optical and SEM images indicate a sheetlike morphology (Figure S9). The solid-state IR spectrum of the material shows the presence of all relevant functional groups (Figure S10). The N−H stretching (2856 cm^{-1}) and bending (1608 cm^{-1}) vibration modes indicate the presence of protonated triethyl amine countercation in the structure.[38] XPS data analysis elucidates the chemical identity and the respective oxidation state. The survey spectra of the as-synthesized material identify the presence of silver, sulfur, oxygen, nitrogen, and fluorine (Figure 3a). The binding energies of Ag $3d_{5/2}$ and Ag $3d_{3/2}$ were observed at 368.15 and 374.15 eV, respectively (Figure 3b), which indicates silver in their +1 oxidation state. The −1 oxidation state of sulfur atoms was determined from its binding energy of 162.5 ($2p_{3/2}$) and 163.7 eV ($2p_{1/2}$), and the deconvolution spectra of C, F, O, and N can be referred to in Figure S11. The absorption spectra of Ag_{10} CAM dispersed in DMAc solution showed a broad band at ∼350 nm (Figure S12). These transitions could be attributed to the LMMCT transition (S→ Ag) mixed with the metal-centered (ds/dp) state.[30]

https://doi.org/10.1021/acs.cgd.4c00322
Cryst. Growth Des. 2024, 24, 4213−4219

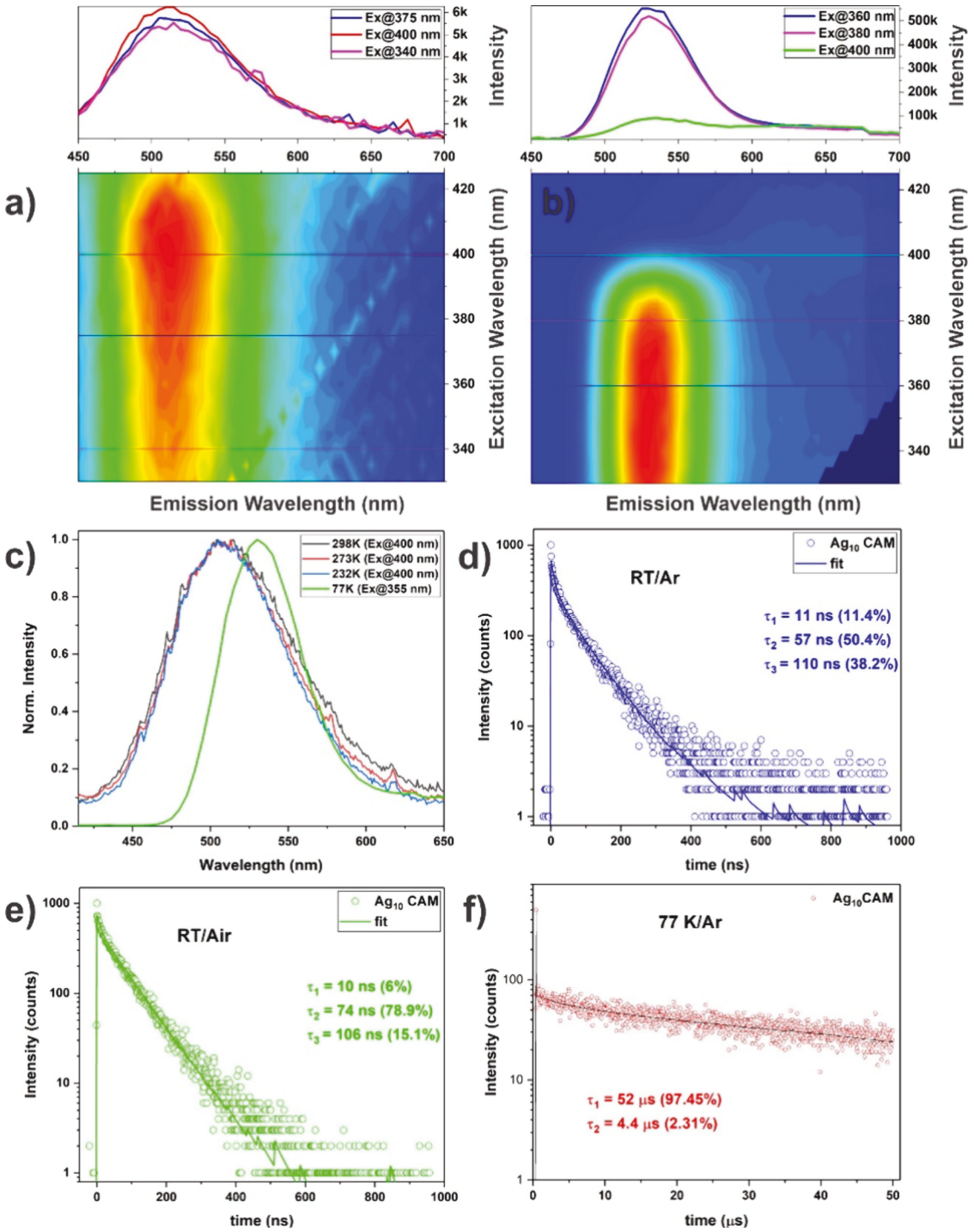

Figure 4. Photophysics of Ag_{10} CAM showing a temperature-dependent singlet−triplet switch: excitation emission mapping at (a) 298 and (b) 77 K; (c) emission profiles recorded at various noted temperatures; transient emission profiles collected at (d) 298 K in argon, (e) 298 K in air, and (f) 77 K in argon (λ_{ex}: 403 nm, λ_{probe}: 512 nm (RT), 530 nm (77 K)).

To understand how the unique close-packed assembly of the Ag_{10} CAM influences their photophysical behavior, steady-state and time-resolved emission spectra were recorded in deaerated DMAc solvent. Steady-state emission spectra (Figure 4a) collected at room temperature (RT) evinced a broad and flat excitation range (340−420 nm), resulting in emission at *ca.* 510 nm (full width at half-maximum, fwhm = 3820 cm^{-1}) and a poor emission QY of 0.19%. In contrast, data collected at 77 K (Figure 4b) display an intense (100× compared to that was measured at RT) and narrow emission band (fwhm = 2190 cm^{-1}) peaking at 530 nm (0.1 eV red-shifted compared to that measured at RT). Red-shift in the emission maxima as the temperature is lowered can be commonly observed in silver-based structures which is due to the contraction of Ag---Ag interactions at lower temperatures thus lowering the cluster-centered triplet state.[39,40] The table S3 comparing the photophysics of the 1D CAM in the literature, provides information about the photophysical behavior and its origin in the assembled structures. Further, to rule out any solvent effect on the PL of Ag_{10} CAM, solid-

https://doi.org/10.1021/acs.cgd.4c00322
Cryst. Growth Des. 2024, 24, 4213−4219

state emission on the powder sample was taken (Figure S13), which matches well with the compound dispersed in DMAc. Temperature-dependent emission profiles (Figure 4c) suggest that lowering the temperature from 298 to 232 K did not alter the population of the main emissive state, which occurred at some temperature between 232 and 77 K. Fitting of the time-resolved emission kinetic profiles provided emission lifetime: at room temperature, the major component has an average $\tau \approx$ 80 ns (Figure 4d, 57.1 ns (50.3%) and 109.9 ns (38.2%)). This time constant was merely affected by the presence of molecular oxygen (τ = 88 ns; Figure 4e, an average of 73.6 ns (78.9%) and 106.3 ns (15.2%)), indicating a singlet emissive population.[41] At room temperature, the existence of triplets was not supported by singlet oxygen generation (Figure S14).[42−44] This suggests that either triplets are not formed or they do not persist long enough for O_2 diffusion. Assuming that the ΔE_{ST} and the intersystem crossing (ISC) efficiency (i.e., spin−orbit coupling) are largely insensitive to temperature, a possible scenario of the temperature-dependent singlet−triplet population can be perceived for such a system with an efficient ISC and a small $S_1 \leftrightarrow T_1$ gap ($\lesssim$ 0.4 eV). At higher temperatures, a reverse ISC (RISC) from $T_1 \rightarrow S_1$ leading to a large singlet population can explain the observed phenomena; such a process may also be facilitated by the crystal vibration of the assembly. For that, at low temperature (77 K), the intense red-shifted emission (Figure 4b; 100× relative to the RT emission) can be assigned to phosphorescence with a lifetime $\tau \approx$ 52 μs (Figure 4f) due to a ceased RISC. Nonetheless, no delayed singlet emission originating from triplet−triplet annihilation was observed.

The moderate $S_1 \leftrightarrow T_1$ gap of ∼0.1 eV was obtained from the energy difference from the room temperature, and the 77 K emission profile is in line with the finding that in the range of 298−232 K, no temperature-dependent gradual peak shift was seen. A gradual peak shift may be expected in a system with a small ΔE_{ST} in the temperature range where thermal variation alters the relative population of the two spin states. This suggests that framework motion may play a role in accessing this moderate gap during the RISC process and that a higher energy singlet state can be completely accessed below 232 K.

4. CONCLUSIONS

We have prepared Ag_{10} CAM by interconnecting $[Ag_{10}(^tBuS)_6(CF_3COO)_6]^{2-}$ cluster unit by 4,4′-trimethylene dipyridine (TMD) linkers. Structural analysis establishes that the CAM is constructed from an *AAAA* (in the *c* direction) and *ABAB*-stack (in the *a* direction) of 1D ladder-shaped "thread" to a three-dimensionally extended supramolecular solid. Spectroscopic analysis indicates its emissive nature at RT, peaking at 510 nm, and a lifetime of $\tau \approx$ 80 ns. Lowering the temperature enhanced the emission intensity (100×), with a peak shifting to 530 nm and a longer lifetime of $\tau \approx$ 52 μs, suggesting its phosphorescent origin. The moderate $S_1 \leftrightarrow T_1$ gap of ∼0.1 eV (due to 1D assembly) suggests an efficient temperature-dependent reverse intersystem crossing defining optical properties where no triplet-based activity was observed near room temperature but exclusive triplet-derived emission at 77 K. These findings highlight the potential of such a platform with a large window of modular emission QY and tunable lifetime as a function of external stimuli like temperature, the extent of which may be modulated by the topology of the assembled structure.

■ ASSOCIATED CONTENT

Supporting Information

The Supporting Information is available free of charge on the ACS Publications Web site. The Supporting Information is available free of charge at https://pubs.acs.org/doi/10.1021/acs.cgd.4c00322.

Details of single crystal structural parameters, cluster structures, silver binding modes, Structural comparison between Ag_{10} CAM and Ag_{10} NC, figures of stacking pattern, PXRD, IR data, XPS data, optical microscopy and scanning electron microscopy images, UV−vis spectra, solid-state emission at 77 K, singlet oxygen emission,Comparison Table of reported 1D CAM and References (PDF)

Accession Codes

CCDC 2301606 contains the supplementary crystallographic data for this paper. These data can be obtained free of charge via www.ccdc.cam.ac.uk/data_request/cif, or by emailing data_request@ccdc.cam.ac.uk, or by contacting The Cambridge Crystallographic Data Centre, 12 Union Road, Cambridge CB2 1EZ, UK; fax: +44 1223 336033.

■ AUTHOR INFORMATION

Corresponding Authors

Pravas Deria − *School of Chemistry, Southern Illinois University-Carbondale, Carbondale 62901, United States;* orcid.org/0000-0001-7998-4492; Email: pderia@siu.edu

Sukhendu Mandal − *School of Chemistry, Indian Institute of Science Education and Research Thiruvananthapuram, Thiruvananthapuram, Kerala 69551, India;* orcid.org/0000-0002-4725-8418; Email: sukhendu@iisertvm.ac.in

Authors

Rahul Ramachandran Manikkoth − *School of Chemistry, Indian Institute of Science Education and Research Thiruvananthapuram, Thiruvananthapuram, Kerala 69551, India*

Priyadarshini Baidya − *School of Chemistry, Indian Institute of Science Education and Research Thiruvananthapuram, Thiruvananthapuram, Kerala 69551, India*

Sreehari Surendran Rajasree − *School of Chemistry, Southern Illinois University-Carbondale, Carbondale 62901, United States*

Priyanka Chandrashekar − *School of Chemistry, Indian Institute of Science Education and Research Thiruvananthapuram, Thiruvananthapuram, Kerala 69551, India*

Manju P. Maman − *School of Chemistry, Indian Institute of Science Education and Research Thiruvananthapuram, Thiruvananthapuram, Kerala 69551, India*

Complete contact information is available at: https://pubs.acs.org/10.1021/acs.cgd.4c00322

Author Contributions

[§]P.B., S.S.R., and P.C. made equal contributions to this work

Author Contributions

The manuscript has been written by combining the contributions of all authors. All authors have approved the final version of the manuscript.

https://doi.org/10.1021/acs.cgd.4c00322
Cryst. Growth Des. 2024, 24, 4213−4219

Notes

The authors declare no competing financial interest.

■ ACKNOWLEDGMENTS

P.D. acknowledges funding from the U.S. National Science Foundation (NSF CAREER CHE-1944903). P.C. acknowledges the Council of Scientific & Industrial Research India for fellowship. The authors are thankful to Dr. Subhrajyoti Bhandary and Dr. Noohul Alam for their assistance in single crystal data solutions and graphical illustration, respectively.

■ REFERENCES

(1) Jin, R.; Zeng, C.; Zhou, M.; Chen, Y. Atomically Precise Colloidal Metal Nanoclusters and Nanoparticles: Fundamentals and Opportunities. *Chem. Rev.* **2016**, *116* (18), 10346−10413.

(2) Chakraborty, I.; Pradeep, T. Atomically Precise Clusters of Noble Metals: Emerging Link between Atoms and Nanoparticles. *Chem. Rev.* **2017**, *117* (12), 8208−8271.

(3) Kang, X.; Zhu, M. Tailoring the Photoluminescence of Atomically Precise Nanoclusters. *Chem. Soc. Rev.* **2019**, *48* (8), 2422−2457.

(4) Chen, T.; Lin, H.; Cao, Y.; Yao, Q.; Xie, J. Interactions of Metal Nanoclusters with Light: Fundamentals and Applications. *Adv. Mater.* **2022**, *34* (25), 2103918.

(5) Matus, M. F.; Häkkinen, H. Understanding Ligand-Protected Noble Metal Nanoclusters at Work. *Nat. Rev. Mater.* **2023**, *8* (6), 372−389.

(6) Antoine, R.; Broyer, M.; Dugourd, P. Metal Nanoclusters: From Fundamental Aspects to Electronic Properties and Optical Applications. *Sci. Technol. Adv. Mater.* **2023**, *24* (1), 2222546 DOI: 10.1080/14686996.2023.2222546.

(7) Joshi, C. P.; Bootharaju, M. S.; Bakr, O. M. Tuning Properties in Silver Clusters. *J. Phys. Chem. Lett.* **2015**, *6* (15), 3023−3035.

(8) Yang, J.; Jin, R. Advances in Enhancing Luminescence of Atomically Precise Ag Nanoclusters. *J. Phys. Chem. C* **2021**, *125* (4), 2619−2625.

(9) Yang, J.; Jin, R. New Advances in Atomically Precise Silver Nanoclusters. *ACS Mater. Lett.* **2019**, *1* (4), 482−489.

(10) Jin, Y.; Zhang, C.; Dong, X. Y.; Zang, S. Q.; Mak, T. C. W. Shell Engineering to Achieve Modification and Assembly of Atomically-Precise Silver Clusters. *Chem. Soc. Rev.* **2021**, *50* (4), 2297−2319.

(11) Ebina, A.; Hossain, S.; Horihata, H.; Ozaki, S.; Kato, S.; Kawawaki, T.; Negishi, Y. One-, Two-, and Three-Dimensional Self-Assembly of Atomically Precise Metal Nanoclusters. *Nanomaterials* **2020**, *10*, 1105 DOI: 10.3390/nano10061105.

(12) Yu, J.; Li, X.; Deria, P. Light-Harvesting in Porous Crystalline Compositions: Where We Stand toward Robust Metal-Organic Frameworks. *ACS Sustain. Chem. Eng.* **2019**, *7* (2), 1841−1854.

(13) Li, X.; Yu, J.; Gosztola, D. J.; Fry, H. C.; Deria, P. Wavelength-Dependent Energy and Charge Transfer in MOF: A Step toward Artificial Porous Light-Harvesting System. *J. Am. Chem. Soc.* **2019**, *141* (42), 16849−16857.

(14) Nakatani, R.; Biswas, S.; Irie, T.; Niihori, Y.; Das, S.; Negishi, Y. Unlocking the Potential of an Atom-Precise Ag_{12} Cluster Assembled Material as a Highly Efficient SERS Sensor for the Detection of Hg^{2+} Ions. *ACS Mater. Lett.* **2024**, *6* (2), 438−445.

(15) Sakai, J.; Biswas, S.; Irie, T.; Mabuchi, H.; Sekine, T.; Niihori, Y.; Das, S.; Negishi, Y. Synthesis and Luminescence Properties of Two Silver Cluster-Assembled Materials for Selective Fe^{3+} Sensing. *Nanoscale* **2023**, *15* (29), 12227−12234.

(16) Li, Y.-H.; Huang, R.-W.; Luo, P.; Cao, M.; Xu, H.; Zang, S.-Q.; Mak, T. C. W. 1D Silver Cluster-Assembled Materials Act as a Platform for Selectively Erasable Photoluminescent Switch of Acetonitrile. *Sci. China Chem.* **2019**, *62* (3), 331−335.

(17) Huang, R. W.; Wei, Y. S.; Dong, X. Y.; Wu, X. H.; Du, C. X.; Zang, S. Q.; Mak, T. C. W. Hypersensitive Dual-Function Luminescence Switching of a Silver-Chalcogenolate Cluster-Based Metal-Organic Framework. *Nat. Chem.* **2017**, *9* (7), 689−697.

(18) Hossain, S.; Imai, Y.; Motohashi, Y.; Chen, Z.; Suzuki, D.; Suzuki, T.; Kataoka, Y.; Hirata, M.; Ono, T.; Kurashige, W.; Kawawaki, T.; Yamamoto, T.; Negishi, Y. Understanding and Designing One-Dimensional Assemblies of Ligand-Protected Metal Nanoclusters. *Mater. Horizons* **2020**, *7* (3), 796−803.

(19) Huang, R. W.; Dong, X. Y.; Yan, B. J.; Du, X. S.; Wei, D. H.; Zang, S. Q.; Mak, T. C. W. Tandem Silver Cluster Isomerism and Mixed Linkers to Modulate the Photoluminescence of Cluster-Assembled Materials. *Angew. Chemie - Int. Ed.* **2018**, *57* (28), 8560−8566.

(20) Alhilaly, M. J.; Huang, R. W.; Naphade, R.; Alamer, B.; Hedhili, M. N.; Emwas, A. H.; Maity, P.; Yin, J.; Shkurenko, A.; Mohammed, O. F.; Eddaoudi, M.; Bakr, O. M. Assembly of Atomically Precise Silver Nanoclusters into Nanocluster-Based Frameworks. *J. Am. Chem. Soc.* **2019**, *141* (24), 9585−9592.

(21) Claridge, S. A.; Castleman, A. W.; Khanna, S. N.; Murray, C. B.; Sen, A.; Weiss, P. S. Cluster-Assembled Materials. *ACS Nano* **2009**, *3* (2), 244−255.

(22) Kang, X.; Zhu, M. Intra-Cluster Growth Meets Inter-Cluster Assembly: The Molecular and Supramolecular Chemistry of Atomically Precise Nanoclusters. *Coord. Chem. Rev.* **2019**, *394*, 1−38.

(23) Bonacchi, S.; Antonello, S.; Dainese, T.; Maran, F. Atomically Precise Metal Nanoclusters: Novel Building Blocks for Hierarchical Structures. *Chem. - A Eur. J.* **2021**, *27* (1), 30−38.

(24) Rival, J. V.; Mymoona, P.; Lakshmi, K. M.; Nonappa; Pradeep, T.; Shibu, E. S. Self-Assembly of Precision Noble Metal Nanoclusters: Hierarchical Structural Complexity, Colloidal Superstructures, and Applications. *Small* **2021**, *17* (27), 2005718.

(25) Chakraborty, P.; Nag, A.; Sugi, K. S.; Ahuja, T.; Varghese, B.; Pradeep, T. Crystallization of a Supramolecular Coassembly of an Atomically Precise Nanoparticle with a Crown Ether. *ACS Materials Lett.* **2019**, *1* (5), 534−540.

(26) Wang, Z. Y.; Wang, M. Q.; Li, Y. L.; Luo, P.; Jia, T. T.; Huang, R. W.; Zang, S. Q.; Mak, T. C. W. Atomically Precise Site-Specific Tailoring and Directional Assembly of Superatomic Silver Nanoclusters. *J. Am. Chem. Soc.* **2018**, *140* (3), 1069−1076.

(27) Dar, W. A.; Jana, A.; Sugi, K. S.; Paramasivam, G.; Bodiuzzaman, M.; Khatun, E.; Som, A.; Mahendranath, A.; Chakraborty, A.; Pradeep, T. Molecular Engineering of Atomically Precise Silver Clusters into 2D and 3D Framework Solids. *Chem. Mater.* **2022**, *34*, 4703 DOI: 10.1021/acs.chemmater.2c00647.

(28) Wang, J. Y.; Huang, R. W.; Wei, Z.; Xi, X. J.; Dong, X. Y.; Zang, S. Q. Linker Flexibility-Dependent Cluster Transformations and Cluster-Controlled Luminescence in Isostructural Silver Cluster-Assembled Materials (SCAMs). *Chem. - A Eur. J.* **2019**, *25* (13), 3376−3381.

(29) Li, Y. L.; Zhang, W. M.; Wang, J.; Tian, Y.; Wang, Z. Y.; Du, C. X.; Zang, S. Q.; Mak, T. C. W. Photoluminescence Modulation of an Atomically Precise Silver(i)-Thiolate Cluster *via* Site-Specific Surface Engineering. *Dalt. Trans.* **2018**, *47* (42), 14884−14888.

(30) Chandrashekar, P.; Sardar, G.; Sengupta, T.; Reber, A. C.; Mondal, P. K.; Kabra, D.; Khanna, S. N.; Deria, P.; Mandal, S. Modulation of Singlet-Triplet Gap in Atomically Precise Silver Cluster-Assembled Material. *Angew. Chem.* **2024**, *63* (6), e202317345.

(31) Sheldrick, G. M. Crystal Structure Refinement with SHELXL. *Acta Crystallogr. Sect. C Struct. Chem.* **2015**, *71* (Md), 3−8.

(32) Sheldrick, G. M. SHELXT - Integrated Space-Group and Crystal-Structure Determination. *Acta Crystallogr., Sect. A* **2015**, *71* (1), 3−8.

(33) Farrugia, L. J. WinGX and ORTEP for Windows: An Update. *J. Appl. Crystallogr.* **2012**, *45* (4), 849−854.

(34) Dolomanov, O. V.; Bourhis, L. J.; Gildea, R. J.; Howard, J. A. K.; Puschmann, H. OLEX2: A Complete Structure Solution, Refinement and Analysis Program. *J. Appl. Crystallogr.* **2009**, *42* (2), 339−341.

(35) Schmidbaur, H.; Schier, A. Argentophilic Interactions. *Angew. Chemie - Int. Ed.* **2015**, *54* (3), 746−784.

https://doi.org/10.1021/acs.cgd.4c00322
Cryst. Growth Des. 2024, 24, 4213−4219

(36) Doerrer, L. H.; Del Rosario, C.; Fan, A. *1.15 - Metallophilic Interactions*; Reedijk, J.; Poeppelmeier, K. R. B. T.-C. I. C. I. I. I. (Third E., Eds.; Elsevier: Oxford, 2023; pp 665−739.
(37) Shen, Y.-L.; Jin, J.-L.; Xie, Y.-P.; Lu, X. Tert-Butyl Thiol and Pyridine Ligand Co-Protected 50-Nuclei Clusters: The Effect of Pyridines on Ag−SR Bonds. *Dalt. Trans.* **2020**, *49* (36), 12574−12580.
(38) Stuart, B. H. *Infrared Spectroscopy: Fundamentals and Applications*; John Wiley & Sons, 2004.
(39) Yan, Z. H.; Li, X. Y.; Liu, L. W.; Yu, S. Q.; Wang, X. P.; Sun, D. Single-Crystal to Single-Crystal Phase Transition and Segmented Thermochromic Luminescence in a Dynamic 3D Interpenetrated Ag^{I} Coordination Network. *Inorg. Chem.* **2016**, *55* (3), 1096−1101.
(40) Su, Y.-M.; Cao, Z.-Z.; Feng, L.; Xue, Q.-W.; Tung, C.-H.; Gao, Z.-Y.; Sun, D. Thermally Hypsochromic or Bathochromic Emissions? The Silver Nuclei Does Matter. *Small* **2022**, *18* (5), 2104524 DOI: 10.1002/smll.202104524.
(41) A relatively faster component of ∼10 ns was observed for both aerobic and anaerobic transient emission profiles − possibly stemming from crystal vibration at RT. The most economic explanation for the slight change in the 50−75 ns time constants in argon and air can be a difference in the dielectric screening of surface-bound cluster excitons.
(42) Zhu, C.; Xin, J.; Li, J.; Li, H.; Kang, X.; Pei, Y.; Zhu, M. Fluorescence or Phosphorescence? The Metallic Composition of the Nanocluster Kernel Does Matter. *Angew. Chem.* **2022**, *61*, e202205947.
(43) Song, Y.; Li, Y.; Zhou, M.; Liu, X.; Li, H.; Wang, H.; Shen, Y.; Zhu, M.; Jin, R. Ultrabright $Au@Cu_{14}$ Nanoclusters: 71.3% Phosphorescence Quantum Yield in Non-Degassed Solution at Room Temperature. *Sci. Adv.* **2021**, *7*, eabd2091.
(44) Mukherjee, S.; Chandrashekar, P.; Aby, I. E.; Mittal, S.; Varghese, A.; Pathak, B.; Mandal, S. Quasi-Isomeric Anion-Templated Silver Nanoclusters: Effect of Bulkiness on Luminescence. *J. Phys. Chem. Lett.* **2023**, *14*, 8548−8554.

https://doi.org/10.1021/acs.cgd.4c00322
Cryst. Growth Des. 2024, 24, 4213−4219